Eur. Phys. J. B **44**, 455–467 (2005)
DOI: 10.1140/epjb/e2005-00145-0

THE EUROPEAN PHYSICAL JOURNAL B

Zero field Wigner crystal

R. Chitra[1,a] and T. Giamarchi[2,b]

[1] Laboratoire de Physique Theorique des Liquides, UMR 7600, Universite de Pierre et Marie Curie, Jussieu, 75005 Paris, France
[2] University of Geneva, 24 Quai Ernest Ansermet, 1211 Geneva, Switzerland

Received 7 September 2004
Published online 30 May 2005 –

Abstract. A candidate for the insulating phase of the 2D electron gas, seen in high mobility 2D MOSFETS and heterojunctions, is a Wigner crystal pinned by the incipient disorder. With this in view, we study the effect of collective pinning on the physical properties of the crystal formed in zero external magnetic field. We use an elastic theory to describe to long wavelength modes of the crystal. The disorder is treated using the standard Gaussian variational method. We calculate various physical properties of the system with particular emphasis on their density dependence. We revisit the problem of compressibility in this system and present results for the compressibility obtained via effective capacitance measurements in experiments using bilayers. We present results for the dynamical conductivity, surface acoustic wave anomalies and the power radiated by the crystal through phonon emission at finite temperatures.

PACS. 71.10.-w Theories and models of many-electron systems – 73.20.Qt Electron solids

1 Introduction

The question of the combined effects of disorder and interactions in correlated electron systems is one of the more important issues in solid state physics. The interest in this longstanding problem has been revived by the spectacular experimental results on the two dimensional electron gas [1]. From a theoretical standpoint, both disorder and interactions are challenges in themselves. By starting from the noninteracting limit, considerable progress was achieved in the understanding of the effects engendered by disorder in the system. The rationale behind such a limit stems from the expectation that not too strong interactions will lead to a Fermi liquid behavior, at least in high dimensions, and therefore, excitations of the system will behave as free fermions. For non interacting electrons in one and two dimensions, disorder is known to lead to the phenomenon of Anderson localization where, all states are localized [2–4]. Going from this non interacting limit to the interacting system has proven quite challenging. In three or higher dimensions, where Fermi liquid theory is expected to hold in the absence of disorder, a renormalization group study [5,6] indicated that disorder strongly enhanced the interactions hence pushing the system away from the noninteracting point. In low dimensions, the situation is even more complicated because in this case, even in the absence of disorder, the interactions themselves have singular effects on the system, and can lead to non fermi liquid phases. For example, in one dimension, where the interacting system is known to be a Luttinger liquid [7,8], the combined effect of disorder and interactions have been shown to lead to behaviors quite different from that anticipated for a noninteracting system [9].

Two dimensions is thus from this point of view doubly marginal: first, the effect of interactions even in the pure system is far from being completely settled and secondly, the disorder, although it leads to localization for the noninteracting system does it only marginally. It is therefore, natural to expect that interactions can alter this picture of marginally localized states. Consequently, the nature of the phase diagram of the two dimensional electron gas as a function of the disorder strength and interactions has been a subject of intense debate. There is however, one limit where the combined effect of interaction and disorder is amenable to an analytical study. This is the limit of strong interactions, where, the electrons in the pure system localize around the sites of a triangular lattice to form a Wigner crystal [10,11]. In this crystal, and far enough from melting, the particles become discernible by their position. Thus quantum effects are simple and manifest themselves in the quantification of the vibrations of the electronic crystal. When a disorder potential is added, its effect is to pin the elastic crystal [12]. The pinning of elastic structures, both classical [13–15] and quantum [16,17], by disorder has been the subject of intense studies and various methods have been developed to tackle these problems. These tools have been used to study the magnetic field induced Wigner crystal formation in the 2D electron gas [18–22]. The optical conductivity

[a] e-mail: chitra@lptl.jussieu.fr
[b] e-mail: Thierry.Giamarchi@physics.unige.ch

and Hall coefficients [19,21] were computed and found to be in excellent qualitative agreement with the experimental observations [23,24]. Combined with the theoretical analysis, the optical conductivity provided clear evidence that for certain filling fractions, the phase realized in this system was indeed a Wigner crystal, weakly pinned on impurities.

The formalism used to study the strong field crystal can be easily modified to obtain the properties of the $B = 0$ crystal. This is of importance [25] to experiments on ultra clean Ga-As heterojunctions and Si MOSFETS which exhibit the zero field metal-insulator transition. A better way to parametrize the system is through the dimensionless parameter $r_s = a/a_B$, where the lattice spacing a is related to the electron density $n = 1/\pi a^2$ and a_B is the Bohr radius of the electron in the 2D electron gas. One of the important questions is whether the insulating phase seen in these systems at low densities or large r_s is indeed a disordered Wigner crystal. In the present paper we focus on analyzing the physical properties of a putative Wigner crystal phase. Our approach complements the standard approach starting from the noninteracting limit. We investigate the effects of the disorder on such a system and compute various observable quantities.

The plan of the paper is as follows. In Section 2 we first use a variational wave function to estimate the effective particle size i.e., size of the localized wave packet at a site. This parameter is expected to play an important role as will be detailed later in the paper. We then present the model and the variational solution. The remainder of the paper is devoted to the computation of various observable quantities: Section 3 deals with the compressibility, Section 4 with the transport properties, in particular, the conductivity, surface acoustic wave absorption and the power radiated by the pinned crystal, followed by a concluding Section 5. Technical details have been relegated to the Appendices.

2 Model and method

We will follow the same procedure outlined in references [19,21]. In the crystal state, the wavefunction of the particles is localized around positions $\mathbf{R}_i$. The wave function has a characteristic width ξ centered around this site. Since the localized wavefunction renders the particles discernible by their position, the crystal can be considered as a collection of discernible particles of size ξ that are labelled by their position $\mathbf{R}_i$. Then only the (quantized) vibrational modes corresponding to the displacements of these particles needs to be retained in any low energy description of the system. Of course, this greatly simplifies the analysis and is the key ingredient which permits a resolution of this problem. As pointed out previously [19,21], there are three important lengthscales to describe the crystal: the lattice spacing a, the size ξ of the particles, and the correlation length of the disorder r_f which we will come back to later. For the case of a strong magnetic field the size of the particle is essentially the cyclotron radius [19,21]. However, for the $B = 0$ Wigner crystal, determining the size of the particle ξ is a question in itself since it is determined by the competition between kinetic energy and interactions.

2.1 Wavefunction in the crystal state

In this section, we use a variational wave function to determine this effective width ξ as a function of the electron density. We choose the ground state to be a Slater determinant of Gaussian wave packets, whose width ξ is chosen to be the variational parameter. The single particle Gaussian wave packets centered around a site i with coordinate $\mathbf{R}_i$, take the form $\psi_i(\mathbf{r}) = \sqrt{\frac{2}{\xi}} \exp -\frac{(\mathbf{r}-\mathbf{R}_i)^2}{\xi^2}$. In the absence of a magnetic field, the total variational energy per site is given by

$$E(\xi) = \frac{\hbar^2}{m\xi^2} + \frac{e^2}{2\epsilon\xi} \sum_i V(\mathbf{R}_i) \tag{1}$$

where the first term is the kinetic energy of the electrons, and the second term is the potential energy arising from coulomb repulsion and

$$V(\mathbf{R}_i) = \exp -\frac{\mathbf{R}_i^2}{4\xi^2} I_0\left(\frac{\mathbf{R}_i^2}{4\xi^2}\right) - \exp -\frac{\mathbf{R}_i^2}{8\xi^2} \tag{2}$$

I_0 is a modified Bessel function of the first kind and $\mathbf{R}_i$ denotes the lattice sites. m, e and ϵ denote the mass, charge and dielectric constant respectively. Minimizing the energy E with respect to ξ results in a self-consistent equation for ξ. Except in the limit of low densities, where one can obtain an analytic expression for ξ, this variational equation is rather complicated to solve analytically for arbitrary densities, thereby requiring the use of numerical techniques. In this paper, we discuss only the low density limit or equivalently the deep crystalline phase. In this limit, as the density is lowered, the effective distance between neighboring sites increases as $a = \sqrt{1/\pi n}$ and the effective width of the wave packet increases in manner such that $a/\xi \gg 1$. Therefore, it is sufficient to retain only the term $\mathbf{R}_i^2 = a^2$ in the expression for V. Expanding the exponential in ξ/a, we obtain following expression for the energy for low densities:

$$E = \frac{\hbar^2}{m\xi^2} + C\frac{e^2\xi^2}{\epsilon a^3} + \ldots \tag{3}$$

The constant C depends on the coordination number of the lattice and the number of terms retained in the sum. Retaining only nearest neighbor sites on a triangular lattice, we obtain $C \simeq 1.88$. Minimization of E with respect to ξ, yields the result,

$$\xi = \left(\frac{a_B}{C}\right)^{\frac{1}{4}} a^{\frac{3}{4}} \equiv n^{-3/8} \tag{4}$$

$a_B = \frac{\epsilon\hbar^2}{me^2}$ is the Bohr radius of the electron. Note that despite the fact that ξ *increases* with decreasing density, the ratio $\xi/a \sim n^{\frac{1}{8}}$ *decreases* with decreasing density in

accord with the assumptions made above, thereby justifying the expansion (3). We emphasize that this result is valid only deep in the crystalline phase. Close to melting, exchange terms become important and we need to solve the equation with the full V to obtain a reasonable variation of the effective particle size with density. Moreover, when exchange terms become non-negligible, the very hypothesis of having discernable particles collapses, and an effective theory different from the one presented in the ensuing section is required.

In the presence of a magnetic field, the same calculation can be done to obtain ξ as a function of the density and the field. For the purely Gaussian wave packet, the magnetic field contributes a term $m\omega_c^2\xi^2/2$ to the energy per site. In the limit of ultra strong magnetic fields dominating the coulomb repulsion, we recover the result that $\xi = \sqrt{\frac{\hbar}{eB}}$ which is just the cyclotron length. For arbitrary fields,

$$\xi = \left[\frac{\hbar^2}{m^2\omega_c^2 + Cme^2/\epsilon a^3}\right]^{\frac{1}{4}}. \tag{5}$$

However, the very assumption of a Gaussian wave packet implies that the electrons are confined to the lowest Landau level and hence the above result holds, strictly speaking, only for strong magnetic fields, and should be viewed as a convenient interpolation formula.

2.2 Elastic Hamiltonian

Now that we have the important parameters characterizing the crystal, we present the elastic Hamiltonian describing the crystal phase. We use the same recipe as outlined in references [19,21], and recall only the main steps here. In the crystalline phase, the electrons occupy the sites of a triangular lattice with a lattice constant a which is related to the density of electrons by $n \sim (\pi a^2)^{-1}$. A particle at a site i is displaced from its mean equilibrium position denoted by $\mathbf{R}_i$, by $\mathbf{u}(\mathbf{R}_i, t)$. In the continuum limit, the vibration modes of the crystal lead to the following elastic action in Fourier space

$$\begin{aligned} S = \frac{1}{2\beta}\sum_{\omega_n}\int d^2q \big[& u_T(\mathbf{q},\omega_n)(\rho_m\omega_n^2 + \Omega_T(\mathbf{q}))u_T(-\mathbf{q},-\omega_n) \\ & + u_L(\mathbf{q},\omega_n)(\rho_m\omega_n^2 + \Omega_L(\mathbf{q}))u_L(-\mathbf{q},-\omega_n)\big] \\ & + \int d^2r d\tau V(\mathbf{r})\rho(\mathbf{r}) \end{aligned} \tag{6}$$

where the transverse (longitudinal) displacements u_T (u_L) are related to the Cartesian displacement $\mathbf{u}$ as follows:

$$u_\alpha(\mathbf{q}) = u^L(\mathbf{q})\hat{\mathbf{q}}_\alpha + u^T(\mathbf{q})\epsilon_{\alpha\beta}\hat{\mathbf{q}}_\beta \tag{7}$$

$\hat{\mathbf{q}} = \mathbf{q}/|\mathbf{q}|$ is the unit vector along $\mathbf{q}$ and $\epsilon_{\alpha\beta}$ is the fully antisymmetric tensor with $\epsilon_{xy} = 1$. These two modes can be interpreted as the shear (u_T) and the compression (u_L) modes respectively. The Matsubara frequencies are $\omega_n = \frac{2\pi n}{\hbar\beta}$ with $\beta = 1/T$ being the inverse temperature. The terms quadratic in the frequency represent the kinetic energy of these modes. $\rho_m = \frac{m}{\pi a^2}, \rho_c = \frac{e}{\pi a^2}$ are the mass and charge densities respectively. The elastic energies of these modes are given [26] by

$$\begin{aligned} \Omega_L(\mathbf{q}) &= d_L|\mathbf{q}| + c_L\mathbf{q}^2 \\ \Omega_T(\mathbf{q}) &= c_T\mathbf{q}^2 \end{aligned} \tag{8}$$

where c_L, c_T, d are elastic constants and, ϵ_0 is the dielectric constant of the substrate. For the classical crystal on the triangular lattice, one has [26] $c_L = -0.18\frac{\rho_c^2 a}{\epsilon_0}$, $c_T = 0.04\frac{\rho_c^2 a}{\epsilon_0}$ and $d = \frac{\rho_c^2}{\epsilon_0}$. These values for the elastic modulii in (8), are valid only for low densities, deep in the crystal phase. For arbitrary densities, the elastic constants depend on the scale ξ and change drastically as one approaches melting. This point should be taken into account while comparing theoretical results for the density dependence of various quantities, with experiments. Unfortunately a rigorous estimate of the elastic constants as a function of the density is still lacking. The linear $\mathbf{q}$ dependence in the compression mode $\Omega_L(\mathbf{q})$ arises from the coulomb repulsion. This is because a longitudinal deformation changes the density profile of the crystal which costs Coulomb energy. On the contrary, transverse modes can be excited without changing the density and are thus purely elastic.

Finally, the last term in the action describes the coupling to disorder, modelled here by a random potential V. The density of the particles $\rho(\mathbf{r})$ is given by

$$\rho(\mathbf{r}) = \sum_i \overline{\delta}(\mathbf{r} - \mathbf{R}_i - \mathbf{u}_i) \tag{9}$$

where $\overline{\delta}$ is a δ-like function of range ξ. Since the disorder can vary at a lengthscale which can a priori be shorter or comparable to the lattice spacing a, the continuum limit $\mathbf{u}(\mathbf{R}_i) \to \mathbf{u}(\mathbf{r})$, valid in the elastic limit $|\mathbf{u}(\mathbf{R}_i) - \mathbf{u}(\mathbf{R}_{i+1}) \ll a$, should be taken with care in the disorder term [27,28]. This is done using the decomposition of the density in terms of its Fourier components

$$\rho(\mathbf{r}) \simeq \rho_0 - \rho_0\nabla\cdot\mathbf{u} + \rho_0\sum_{\mathbf{K}\neq 0} e^{iK\cdot(\mathbf{r}-\mathbf{u}(\mathbf{r}))} \tag{10}$$

where ρ_0 is the average density and $\mathbf{K}$ are the reciprocal lattice vectors of the crystal.

The above formula shows that one should distinguish between various parts of the disorder. Disorder that varies at lengthscales much larger than the lattice spacing couples only to the $\rho_0\nabla\cdot u$ term. Although such a term can modify the structure of the crystal quite strongly, it does not lead to pinning and disappears from the transport properties. Pinning, and thus the dominant contribution to transport coefficients, is however achieved by the disorder that varies on lengthscales comparable to the lattice spacing. In heterojunctions, such a disorder is expected to be present due to interface roughness arising from epitaxial growth of the semiconducting layers sandwiching the electron gas. The real system is further complicated by the

presence of a long range disorder potential arising from the presence of ineffectively screened dopants outside the plane of the electron gas. However such a disorder varies slowly compared to the scale of the lattice spacing, and we will thus assume that we can neglect it as far as the transport properties are concerned. Moreover, if the disorder is weak and leads to collective pinning one can assume a Gaussian distribution for V, since each volume of the system will average over a large number of independent impurities. In this case,

$$\overline{V(\mathbf{r})V(\mathbf{r}')} = \Delta_{r_f}(\mathbf{r}-\mathbf{r}') \tag{11}$$

where Δ_{r_f} is effectively a delta function with a range r_f, which is the correlation length of the disorder. As discussed in reference [21], taking into account such a finite correlation length for the disorder can also be done by taking a delta-function correlated disorder but replacing the size of the particles ξ by $\xi_0 \sim \max(r_f, \xi)$ in $\overline{\delta}$ in (9).

2.3 Gaussian variational method

We treat (6) using a variational method [19,29]. We present here only the main steps of the treatment and refer the reader to reference [21] for details. Many of the technical details and subtleties of the method can be found in the literature (see e.g. Refs. [16,30] for a review). We first average (6) over disorder by introducing replicas. This averaging results in an effective action which involves interactions between the n replicas, given by

$$\begin{aligned} S = \frac{1}{2}\sum_{\omega_n}\int_{\mathbf{q}}\sum_a u_T^a(\mathbf{q},\omega_n)\left[\rho_m\omega_n^2 + \Omega_T(\mathbf{q})\right]u_T^a(-\mathbf{q},-\omega_n) \\ + u_L^a(\mathbf{q},\omega_n)\left[\rho_m\omega_n^2 + \Omega_L(\mathbf{q})\right]u_L^a(-\mathbf{q},-\omega_n) \\ - \frac{\rho_0^2}{2}\int d^2r\int_0^\beta\int_0^\beta d\tau d\tau' \\ \times \sum_{a,b,\mathbf{K}} \Delta_K \cos\left[\mathbf{K}\cdot\left(u^a(\mathbf{r},\tau) - u^b(\mathbf{r},\tau')\right)\right]. \end{aligned} \tag{12}$$

The replica indices, a, b run from 1 to n. The physical disorder averages are recovered in the limit $n \to 0$. As discussed above, the size of the particles ξ and the finite correlation length of the disorder r_f broaden the delta function in the density (9) over a size ξ_0. Consequently the sum over K in (10) can be restricted to values of K smaller than $K_{\max} \sim \pi/\xi_0$. This in conjunction with the local nature of the disorder permits us to replace Δ_K in (12) as a constant $\Delta_K = \Delta$ for $K < K_{\max}$ and zero otherwise.

We now search for a variational solution to (12) by using the best quadratic action approximating (12). We use the trial action

$$S_0 = \frac{1}{2\beta}\int_{\mathbf{q}}\sum_{n,\mu,\nu} u_\mu^a(\mathbf{q},\omega_n)(G^{-1})_{\mu\nu}^{ab}(\mathbf{q},\omega_n)u_\nu^b(-\mathbf{q},-\omega_n) \tag{13}$$

where the whole Green's function $(G^{-1})_{\mu\nu}^{ab}(\mathbf{q},\omega_n)$ are variational parameters. The variational free energy is now given by

$$F_{\rm var} = F_0 + \langle S - S_0\rangle_{S_0}. \tag{14}$$

The variational parameters are then determined by the saddle point equations

$$\frac{\partial F_{\rm var}}{\partial (G^{-1})_{\mu\nu}^{ab}(\mathbf{q},\omega_n)} = 0. \tag{15}$$

The pertinent solution of these saddle point equations (15) solved in the limit of the number of replicas $n \to 0$, breaks replica symmetry [19,21,29].

The connected Green's functions defined as $(G_c^{-1})_{\mu\nu} = \sum_b (G^{-1})_{\mu\nu}^{ab}$ for the two modes are given by

$$\begin{aligned} G_{cT}(\mathbf{q},i\omega_n) &= \frac{1}{\rho_m\omega_n^2 + \Omega_T(\mathbf{q}) + I(i\omega_n) + \Sigma(1-\delta_{n,0})} \\ G_{cL}(\mathbf{q},i\omega_n) &= \frac{1}{\rho_m\omega_n^2 + \Omega_L(\mathbf{q}) + I(i\omega_n) + \Sigma(1-\delta_{n,0})} \end{aligned} \tag{16}$$

where the disorder induced pseudogap is found to be

$$\Sigma = c_T R_c^{-2} = c_T(2\pi^2)^{-\frac{1}{6}} R_a^{-2}(a/\xi_0)^6 \tag{17}$$

with $\xi_0 = \max[r_f, \xi]$, $c_T \simeq \frac{\rho_c^2 a}{\epsilon_0}$ and $R_a \simeq c_T/\pi n^2\sqrt{\Delta}$. In the present context, R_c and R_a are defined by the two equations above. These two lengthscales are of physical significance within the broader context of pinned elastic structures. The length R_c is the Larkin-Ovchinikov length [31], which corresponds to the distance for which displacements are of the order of the size of the particle (or correlation length of the disorder) $u(R_c) \sim \xi_0$. This is the length above which metastability and pinning appear. The length R_a is the positional length, and corresponds to the distance for which the displacements are of the order of the lattice spacing $u(R_a) \sim a$. See reference [15,19] for further details.

As explained in references [21,29], the function $I(i\omega_n)$ is determined by the following self-consistent equation derived in the semi-classical limit:

$$\begin{aligned} I(i\omega_n) = 2\pi c_T\Sigma\int_{\mathbf{q}}\Bigg[\frac{1}{\Omega_T(\mathbf{q})+\Sigma} + \frac{1}{\Omega_L(\mathbf{q})+\Sigma} \\ - \frac{1}{\Omega_T(\mathbf{q}) + \rho_m\omega_n^2 + I(i\omega_n) + \Sigma} \\ - \frac{1}{\Omega_L(\mathbf{q}) + \rho_m\omega_n^2 + I(i\omega_n) + \Sigma}\Bigg]. \end{aligned} \tag{18}$$

In the limit of small ω_n, the above equation can be solved analytically to obtain

$$I(i\omega_n) = \sqrt{2\rho_m\Sigma\left[1 + \frac{4c_T\Sigma}{d^2}\log\left(\frac{d^2}{c_T\Sigma}\right)\right]}|\omega_n|. \tag{19}$$

This equation for I can be continued to real frequencies and then solved numerically. The solution of the variational equations as obtained above thus allows us to extract numerous physical quantities of the disordered system. We will first discuss the compressibility in the forthcoming section and the transport will be discussed in Section 4.

3 Compressibility

In this section we discuss the compressibility of the pinned Wigner crystal. Although the compressibility is usually simply related to density-density correlations, here one should take special care in defining this quantity due to two complications inherent to the Wigner crystal: (i) for charged systems it is crucial to know whether one keeps the system neutral or not when letting the density fluctuate; (ii) since in presence of disorder one expects glassy properties, the question of the timescale over which the measurements are performed is relevant.

The naive way to define the compressibility κ would be to add to the Hamiltonian the standard chemical potential term

$$H = -\mu \int d^2 r(\rho(\mathbf{r}) - \rho_0) \tag{20}$$

and to compute the average change in density $\langle \rho(\mathbf{r}) - \rho_0 \rangle$. In linear response, the compressibility is given by the density density correlator. Using (7) and (10) the compressibility is directly related to the correlation of the longitudinal displacements. For the pure system this is easily computed to be

$$\kappa \propto \lim_{q \to 0, \omega_n = 0} \frac{q^2}{\omega_n^2 + \Omega_L(\mathbf{q})}. \tag{21}$$

Since $\Omega_L(\mathbf{q}) \propto q$, the compressibility is zero. This arises from the fact that the change of density induced by μ occurs for a constant neutralizing background. The combined system of the crystal plus the background thus becomes charged which costs too much energy and inhibits this kind of density fluctuation.

To have a non-zero compressibility, even for the pure system, it is thus important to change the density of the Wigner crystal, while at the same time changing the background to maintain neutrality. An experimental way of doing this is to perform a capacitance measurement [32]. We show here how to compute such a capacitance for the case of two Wigner crystals planes [33] separated by a distance d, as shown in Figure 1. Though the experimental setup (two layers and a gate) considered in reference [32] is slightly different from the one considered here, we expect the results obtained here to hold for this experimental geometry as well, since the crucial ingredient, namely ensuring the neutrality of the system is preserved. Similar results would be obtained if one of the plates was replaced by a normal metal (such as a top gate for example).

The Hamiltonian of the system depicted in Figure 1 is thus

$$H = H_1^0 + H_2^0 + \frac{1}{2} \sum_{(\alpha,\beta)=1,2} \int_{\mathbf{r},\mathbf{r}'} V_{\alpha\beta}(\mathbf{r} - \mathbf{r}')[\rho_\alpha(\mathbf{r}) - \rho_0][\rho_\beta(\mathbf{r}') - \rho_0] + \frac{\mu}{2} \int_{\mathbf{r}} [\rho_1(\mathbf{r}) - \rho_2(\mathbf{r})] \tag{22}$$

where $H_{1,2}^0$ are the elastic Hamiltonians of each 2DEG excluding the Coulomb interaction. $V_{\alpha\beta}$ is the usual

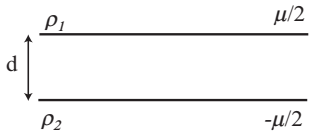

Fig. 1. Capacitance measurement, which gives access to the compressibility of the system. A voltage difference μ is applied to a capacitor. Here for simplicity, the capacitor is made of two planes of the 2DEG.

Coulomb interaction in and between the planes. If one assumes that the system is neutral in the absence of μ, then within linear response, the charge on one plane when a potential μ is applied is

$$\langle \rho_1 \rangle = \frac{\mu}{2}[\langle \rho_1 \rho_1 \rangle - \langle \rho_1 \rho_2 \rangle]. \tag{23}$$

Thus (23) gives directly the capacitance $C = \langle \rho_1 \rangle / \mu$. More generally, we define the capacitance for finite q and ω (e.g. corresponding to a time and space dependent potential μ)

$$C(\omega, \mathbf{q}) = \frac{1}{2}[\langle \rho_1 \rho_1 \rangle_{\omega,\mathbf{q}} - \langle \rho_1 \rho_2 \rangle_{\omega,\mathbf{q}}] \tag{24}$$

where the subscripts $\omega, \mathbf{q}$ indicate that the correlation functions are evaluated for finite momentum and frequency. For a metal, a RPA evaluation of (24) gives back [33] the standard formula for the compressibility of a charged system. We recall the calculation in Appendix A for convenience. One can use this general formula to compute the capacitance for the Wigner crystal. Since one is interested in the limit of small q and ω one can use the decomposition of the density (10). The Hamiltonian (6) becomes

$$H = H_1^{sr} + H_2^{sr} + \frac{\rho_0^2}{2} \sum_{(\alpha,\beta)=1,2} \int_{\mathbf{r},\mathbf{r}'} V_{\alpha\beta}(\mathbf{r} - \mathbf{r}')[\nabla \cdot \mathbf{u}_\alpha(\mathbf{r})][\nabla \cdot \mathbf{u}_\beta(\mathbf{r}')] \tag{25}$$

where $H_{1,2}^{sr}$ is the part of the Hamiltonian that does not contain the *long range* (i.e. for $\mathbf{q} \sim 0$) of the Coulomb interaction. $\mathbf{u}_1$ and $\mathbf{u}_2$ denote the displacement vectors in the two planes. Since $V_{11}(\mathbf{q}) = V_{22}(\mathbf{q}) \propto 1/|\mathbf{q}|$, the third term in (25) obviously yields the part proportional to $\mathbf{q}$ in the bulk modulus for an isolated plane (see (8)). Note that in writing (25) we have neglected the short range part of the interplane interaction

$$H_{1,2}^{SR} = \int_{\mathbf{r},\mathbf{r}'} V_{\alpha\beta}(\mathbf{r} - \mathbf{r}')\rho_0^2 \sum_{\mathbf{K},\mathbf{K}' \neq 0} e^{i\mathbf{K}\cdot(\mathbf{r} - \mathbf{u}_1(\mathbf{r}))} e^{-i\mathbf{K}'\cdot(\mathbf{r}' - \mathbf{u}_2(\mathbf{r}'))}. \tag{26}$$

The translational invariance restricts the sum to $\mathbf{K} = \mathbf{K}'$ terms. This essentially contains the Fourier transform of the interplane potential which using (31) is found to behave as

$$\int_{\mathbf{r}} V_{12}(\mathbf{r}) e^{i\mathbf{K}\cdot\mathbf{r}} = \frac{(2\pi)e^{-Kd}}{K}. \tag{27}$$

$$\begin{pmatrix} \left[\rho_m\omega_n^2 + \Omega_L^{\rm sr}(\mathbf{q}) + \rho_0^2 q^2 V_{11}(\mathbf{q})\right] G_{11} + F[G_{11}] & \rho_0^2 q^2 V_{12}(\mathbf{q}) G_{12} \\ \rho_0^2 q^2 V_{12}(\mathbf{q}) G_{21} & \left[\rho_m\omega_n^2 + \Omega_L^{\rm sr}((\mathbf{q}) + \rho_0^2 q^2 V_{11}(\mathbf{q})\right] G_{22} + F[G_{22}] \end{pmatrix} \tag{35}$$

Thus if the planes are at a distance d much larger than the lattice spacing a of the WC, this term is obviously much smaller than the long range part of the intraplane interaction, and can be neglected. It can also be neglected if one of the planes is an homogeneous electron gas (i.e. a simple metal). In the case where the two planes are close enough this term should be retained and can lead to interesting effects such as the locking of the two Wigner crystals together [34]. The in-plane coupling of the higher harmonics of the density contribute to H^{SR} and generate the regular non-singular part of the Hamiltonian (i.e. the part proportional to q^2 in the elastic coefficients). In fact this approach is synonymous with the method used in reference [26] to calculate the elastic coefficients. The derivation is done in Appendix B.

Let us now use the general formula (24) to compute the capacitance of the pure system. From (10), the long wavelength part of the density is given by

$$\rho_\alpha(\mathbf{q}) = -i\rho_0 q u_{\alpha L}(\mathbf{q}). \tag{28}$$

One thus needs only the longitudinal part of the action to calculate the compressibility.

$$S = \left(u_L^1(\mathbf{q})\ u_L^2(\mathbf{q}) \right) \times \begin{pmatrix} \omega_n^2 + \Omega_L^{\rm sr}(\mathbf{q}) + \rho_0^2 q^2 V_{11}(\mathbf{q}) & \rho_0^2 q^2 V_{12}(\mathbf{q}) \\ \rho_0^2 q^2 V_{12}(\mathbf{q}) & \omega_n^2 + \Omega_L^{\rm sr}(\mathbf{q}) + \rho_0^2 q^2 V_{11}(\mathbf{q}) \end{pmatrix} \times \begin{pmatrix} u_L^1(-\mathbf{q}) \\ u_L^2(-\mathbf{q}) \end{pmatrix} \tag{29}$$

where $\Omega_L^{\rm sr}(\mathbf{q})$ is the "short range" part of the elastic coefficients (8). Using (28) and (24) one obtains the capacitance

$$C(i\omega_n, \mathbf{q}) = \frac{1}{2} \frac{\rho_0^2 q^2}{\rho_m\omega_n^2 + \Omega_L^{\rm sr}(\mathbf{q}) + \rho_0^2 q^2 [V_{11}(\mathbf{q}) - V_{12}(\mathbf{q})]}. \tag{30}$$

The thermodynamic compressibility is given by the value of C for $\omega_n = 0$. Note that in this case one obtains the same value by considering the retarded correlation function (doing the analytic continuation $i\omega_n \to \omega + i\delta$) and taking the limit $\omega \to 0$ first (for a fixed q). The divergence arising from the long range part of the Coulomb potential now cancels since

$$V_{11}(\mathbf{q}) - V_{12}(\mathbf{q}) = \int d^2 r e^{i\mathbf{q}\cdot\mathbf{r}} \left[\frac{1}{r} - \frac{1}{\sqrt{r^2 + d^2}}\right] = \frac{(2\pi)(1 - e^{-qd})}{q} \tag{31}$$

is non divergent when $q \to 0$. This of course traduces the fact that the global system remains neutral when the potential is applied. Using (31) one obtains

$$C(\omega_n = 0, q \to 0) \to \frac{\rho_0^2 q^2}{2\Omega_L^{\rm sr}(\mathbf{q}) + 4\pi d(\rho_0^2 q^2)}. \tag{32}$$

One thus recovers that the inverse capacitance is the sum of a purely geometric term and an electronic one (see (A.4)). The electronic capacitance is simply given by

$$C_{el} = \lim_{q\to 0} \frac{\rho_0^2 q^2}{2\Omega_L^{\rm sr}(q)} = \frac{\rho_0^2}{2c_L} \propto -\frac{\epsilon_0}{e^2 a}. \tag{33}$$

This term, which for a normal metal is simply related to the static compressibility, is thus negative for a Wigner crystal, if one uses the classical estimates [26] for the elastic coefficients. The fact that a system of discrete charges can lead to such effects has been noted before for classical Wigner crystals (see e.g. Ref. [35] and references therein).

Let us now turn to the disordered case. In the presence of disorder, the same calculation can be repeated to obtain the compressibility. To do this, we assume that the disorder potentials in each layer is drawn from independent distributions and repeat the variational calculation of the previous section. The trial action (13) has now two additional indices that denote the two layers. For simplicity, we will only denote these indices here, all the others being implicit. The trial action is thus (in these indices) a two by two matrix with the Green's functions $G^{-1}_{\mu\nu}$ where $\mu, \nu = 1, 2$. Obviously $G_{11} = G_{22}$ and $G_{12} = G_{21}$. From (24) and the inversion of the two by two matrix the capacitance is thus given by

$$C(\omega, \mathbf{q}) = \frac{\rho_0^2 q^2}{2}[G_{11} - G_{12}] = \frac{\rho_0^2 q^2}{2}\left[\frac{1}{G_{11}^{-1} - G_{12}^{-1}}\right] \tag{34}$$

where all other indices (replica, longitudinal, q, ω) are implicit. The variational procedure can now be repeated to determine G_{11} and G_{12}. Because the disorder is independent from plane to plane, the trial free energy has the following matrix structure

see equation (35) above

where F is the same as the term induced by disorder averaging in a single plane. The minimization (15) now gives the self consistent equations

$$\begin{aligned} G_{11}^{-1} &= [\rho_m\omega_n^2 + \Omega_L^{\rm sr}(\mathbf{q}) + \rho_0^2 q^2 V_{11}(\mathbf{q})] + F'[G_{11}] \\ G_{12}^{-1} &= \rho_0^2 q^2 V_{12}(\mathbf{q}). \end{aligned} \tag{36}$$

Note that the in-plane inverse Green's function is identical to the one in the absence of interplane interactions, and thus is given by the variational solution of the previous section. The interplane inverse Green's function is trivial and simply given by the long range part of the interaction between the planes.

$$C(\omega_n, \mathbf{q}) = \frac{1}{2} \frac{\rho_0^2 q^2}{\rho_m \omega_n^2 + \Omega_L^{\rm sr}(\mathbf{q}) + \rho_0^2 q^2 [V_{11}(\mathbf{q}) - V_{12}(\mathbf{q})] + I(i\omega_n) + \Sigma(1 - \delta_{n,0})} \tag{37}$$

In the presence of disorder, the compressibility is given by the connected Green's function [16]. Using (34), (36) and (16) one obtains

see equation (37) above.

As for the pure system, we see that the geometric capacitance contributes to the total capacitance. Isolating the electronic part of the capacitance we find

$$C_{el}(\omega_n, \mathbf{q}) = \frac{\rho_0^2 q^2/2}{\Omega_L^{\rm sr}(\mathbf{q}) + I(i\omega_n) + \Sigma(1 - \delta_{n,0})} \tag{38}$$

(38) thus shows that in the presence of disorder one has to distinguish between the thermodynamic capacitance and the dynamical one. If one considers the thermodynamic capacitance, then (38) should be computed for $\omega_n = 0$. In that case all contributions from the disorder disappear in (38) and the capacitance is identical, within the variational approximation, to that of the pure system. On the other hand, if one considers a capacitance measurement in response to a modulation at finite frequency, which is certainly the case experimentally, one has to take the analytic continuation $i\omega_n \to \omega + i\delta$ first. In this case one obtains

$$C_{el}(\omega, \mathbf{q}) = \frac{\rho_0^2 q^2/2}{\Omega_L^{\rm sr}(\mathbf{q}) + I(\omega) + \Sigma}. \tag{39}$$

As for the pure case, one should take the limit $\omega \to 0$ first. In this limit, the function $I(\omega)$ is regular and tends to zero. Taking $q \to 0$, we see that since the mass term Σ prevails in the denominator the compressibility is zero. This is a consequence of the fact that the pinning by disorder renders the system inflexible to charge modulations. Note that contrary to the pure case, the thermodynamic response and the slow dynamic one are not equivalent in the disordered case. This is not surprising considering the glassy nature of the system.

As for the effect of a magnetic field on the compressibility, naively one would expect that it has no effect since the compressibility is a static property. This is what is found within the variational approximation. However it is important to note that, although there is no explicit magnetic field dependence of the compressibility, there is still a variation of the thermodynamic compressibility with the magnetic field accruing from the field dependence of the elastic constants of the crystal.

4 Transport

We now focus on the consequences of disorder for the zero temperature transport properties. This is of particular importance to the materials which exhibit the zero field metal-insulator transition where transport is indeed the main probe of the physics. Up to now, the experimental emphasis has been on finite temperature resistivity and magneto-resistance measurements. However for the Wigner crystal such quantities are difficult to compute theoretically since they are dominated by the defects in the system [21]. It is thus difficult to use them as a probe of the Wigner crystal nature of the underlying phase. As explained in references [17,21] the optical conductivity does not suffer from such a problem and can be reliably computed theoretically from the elastic Hamiltonian of the crystal. Here, we present results for the dynamical conductivity, surface acoustic wave measurements and the power radiated by the crystal. These measurements done in the quantum Hall samples at high fields were instrumental in clarifying the physics of these systems [23,24,36–38]. Clearly similar measurements are called for in the zero field samples, and would be crucial to understand the physics of the insulating phase.

4.1 Conductivity

The conductivity of the disordered crystal can be obtained from the displacement-displacement correlation function [21] and is given by:

$$\sigma_{\alpha\beta}(\omega) = i\rho_c^2 \omega G_{\alpha\beta}(q = 0, \omega + i\epsilon) \tag{40}$$

where $\mu\nu = x, y$ and $G_{\mu\nu}(\mathbf{q}, \omega) = \langle u_\mu(\mathbf{q}, \omega) u_\nu(\mathbf{q}, \omega) \rangle$ are the displacement Green's function. Since, there is no magnetic field, the longitudinal resistivities $\sigma_{xx}(\omega) = \sigma_{yy}(\omega) = \sigma(\omega)$. These functions are related to the connected Green's functions of (16) and using an analytic continuation $i\omega_n \to \omega + i\epsilon$, we obtain

$$\sigma(\omega) = i\rho_c^2 \frac{\omega}{-\rho_m \omega^2 + \Sigma + I(\omega)}. \tag{41}$$

As seen in other disordered elastic systems [21,29], the conductivity is completely determined by Σ and $I(\omega)$. For the pure crystal, $\Sigma = I(\omega_n) = 0$, and one recovers that the real part of the conductivity exhibits a $\omega = 0$ Drude peak and zero finite frequency conductivity, while the imaginary part varies as $1/\omega$. In the presence of disorder, the crystal is pinned collectively forbidding any sliding motion of the crystal. Consequently, the Drude peak is annihilated and the dc conductivity $\mathrm{Re}\sigma(\omega = 0) = 0$. This results in a non-zero finite frequency conductivity and the appearance of a peak at a new scale $\omega_p \simeq \sqrt{\frac{\Sigma}{\rho_m}}$ called the pinning frequency [39]. The pinning frequency is thus determined by (17). The pinning peak is broadened by the dissipative term $I(\omega)$ which also generates, as can be seen from (41), a slight shift of the pinning peak from ω_p due to the real part of $I(\omega)$. Using (19), we find that for $\omega \ll \omega_p$.

$$\begin{aligned} \mathrm{Re}\sigma(\omega) &\sim \rho_c^2 \sqrt{2\rho_m \Sigma \left[1 + \frac{4 c_T \Sigma}{d^2} \log\left(\frac{d^2}{c_T \Sigma}\right)\right]} \frac{\omega^2}{\Sigma^2} \\ \mathrm{Im}\sigma(\omega) &= \rho_c^2 \frac{\omega}{\Sigma} \end{aligned} \tag{42}$$

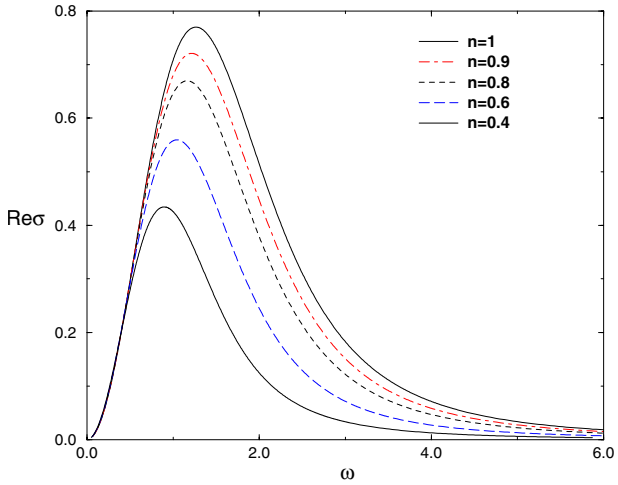

Fig. 2. The real part of the conductivity $\sigma(\omega)$ (in units of $e^2/\sqrt{A_2 m}$) as a function of the frequency measured in units of $\sqrt{\frac{A_2}{m}}$ for the regime where the disorder correlation length $r_f < \xi$ for various electronic densities n(in units of $(\pi a_B^2)^{-1}$). These curves have been obtained using the classical values of the elastic moduli and the parameter A_2 is given in (50).

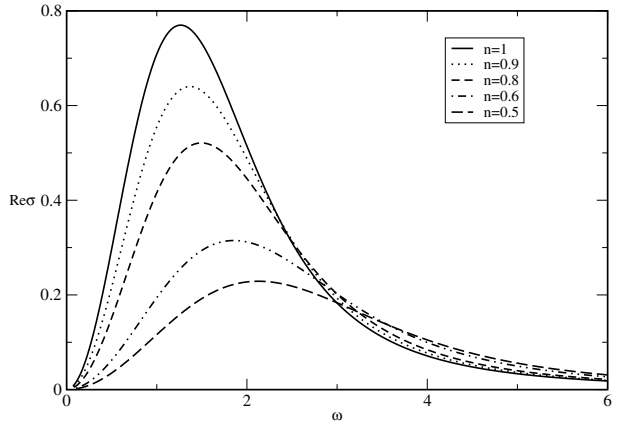

Fig. 3. The real part of the conductivity $\sigma(\omega)$ (in units of $e^2/\sqrt{A_1 m}$) as a function of the frequency measured in units of $\sqrt{\frac{A_1}{m}}$ for the regime where the disorder correlation length $r_f > \xi$ for various densities n (in units of $(\pi a_B^2)^{-1}$). As before, these curves have been obtained using the classical values of the elastic moduli and the parameter A_1 is given in (47).

while for high frequencies $\omega \gg \omega_p$

$$\mathrm{Re}\sigma(\omega) \sim \frac{\rho_c^2}{\rho_m^2 \omega^3}. \tag{43}$$

The behavior of the conductivity for all intermediate values of ω can be obtained by solving numerically (18) and using the solution for $I(\omega)$ in (41). Referring to (17), we note that the result for Σ depends on whether the disorder correlation length is larger or smaller than the size of the particles of the crystal ($r_f \lesseqgtr \xi$). This has serious implications for the density dependence of the conductivity as can be inferred from Figures 2 and 3 where, we plot the conductivity for different values of the density in the two regimes $r_f < \xi$ and $r_f > \xi$.

The density dependence of the pinning frequency and the height of the pinning peak can now be evaluated in a straightforward manner. The peak height is given by the expression

$$P = \sigma(\omega_p) = \rho_c^2 \sqrt{\frac{\Sigma}{\rho_m}} \mathrm{Im} \frac{1}{\mathrm{I}(\omega_\mathrm{p})}. \tag{44}$$

If we neglect corrections to the pinning frequency arising from I, then $I(\omega_p) = \Sigma Z$ where Z is some complex number, and in this case, the leading density dependence of the peak height is given by

$$P \propto \frac{\rho_c^2}{\sqrt{\rho_m \Sigma}}. \tag{45}$$

The behavior of the peak height is thus entirely determined by Σ. To obtain the actual density dependence, one needs to know the elastic moduli of the crystal. Using the results of reference [26], we find that in the regime, $r_f > \xi$, the electrons see the bare disorder and

$$\begin{aligned} \Sigma &= A_1 n^{-\frac{1}{2}} \\ R_c &= \sqrt{\frac{be^2}{A_1 \epsilon \sqrt{\pi}} n} \end{aligned} \tag{46}$$

where

$$A_1 = (2\pi^2)^{-\frac{1}{6}} \Delta\epsilon / b\sqrt{\pi} e^2 r_f^6 \tag{47}$$

and $b = 0.04$ for the classical triangular lattice. This leads to

$$\begin{aligned} \omega_p &\propto n^{-\frac{3}{4}} \\ P &\propto n^{\frac{7}{4}}. \end{aligned} \tag{48}$$

Consequently, the peak position shifts to higher frequencies and the peak height decreases with decreasing density as is seen in Figure 3.

In the opposite regime where the disorder correlation length $r_f < \xi$, the effective particle size being larger, the particle sees an averaged effective disorder. Using the classical values for the elastic moduli, we find that

$$\begin{aligned} \Sigma &= A_2 n^{\frac{7}{4}} \\ R_c &= \sqrt{\frac{be^2}{A_2 \epsilon \sqrt{\pi}}} n^{-\frac{1}{8}} \end{aligned} \tag{49}$$

where

$$A_2 = (2\pi^2)^{-\frac{1}{6}} \Delta\epsilon \pi^{\frac{7}{4}} (C/a_B)^{\frac{3}{2}} / be^2 \tag{50}$$

and $C = 1.88$ for the triangular lattice cf. (3). Hence

$$\begin{aligned} \omega_p &\propto n^{\frac{3}{8}} \\ P &\propto n^{\frac{5}{8}}. \end{aligned} \tag{51}$$

This implies that as density is decreased, the pinning peak shifts to lower frequencies accompanied by a concomitant

decrease of peak height as shown in Figure 2. The density dependence of the pinning peak is a test that can prove whether the insulating phase is indeed a Wigner crystal.

The above results were obtained using the variational approximation (12) which takes into consideration only small oscillations around the pinned position. This method describes the correct physics only if topological defects (solitonic excitations of the system) are unimportant. This is indeed the case in three dimensions, where the Bragg glass phase of a weakly disordered system is stable to the creation of topological defects [28] and the variational results for the conductivity are valid for all frequencies. However, in $d = 2$, topological defects are generated by the disorder albeit at a length scale ξ_D that can be arbitrarily large [28,40,41] compared to the positional length scale R_a (and thus even larger compared to the pinning length R_c). Thus, as explained in detail in reference [21], even in $d = 2$ the existence of topological defects does not affect our results in the range of frequencies around the pinning peak. On the contrary, the d.c. and very low frequency behavior of the conductivity will be affected by the presence of defects. For instance at $T = 0$, the $\sigma \sim \omega^2$ behavior predicted by the variational approach will be replaced by $\sigma \sim |\omega|$ in the presence of defects [42], due to soliton-type excitations. At finite temperatures, in the absence of defects the crystal would be collectively pinned leading to a non linear response and the absence of linear resistivity, whereas a linear resistivity of the variable range hopping (VRH) or Efros-Schklovskii (ES) form is expected [43] when defects are taken into account. Indeed the connection between VRH-ES conductivity and soliton type excitation has been recently made in the framework of disordered elastic systems [44]. We emphasize that though defects have to included in the estimation of the low frequency conductivity, this is not necessary for calculations of the optical conductivity for frequencies around the pinning peak. Since the variational method permits a quantitative computation of the optical conductivity, conductivity measurements can be used as the principal experimental tool to determine the Wigner crystalline nature of insulating states in two dimensional electron gases.

Another interesting quantity is the threshold electric field for depinning of the crystal. This field is related [31] to the parameters of the problem by the relation $E_T = c_T R_c^{-2} \xi_0$ where $\xi_0 = \max[r_f, \xi]$. Using (46, 49), we obtain

$$\begin{aligned} E_T &\propto n^{-\frac{1}{2}}, \quad r_f > \xi \\ E_T &\propto n^{\frac{11}{8}}, \quad r_f < \xi. \end{aligned} \tag{52}$$

Note that for $r_f > \xi$, the threshold field increases with inverse density, implying that the crystal gets more and more pinned in the low density regime. However, since ξ increases when the density decreases according to (4) on has to crossover to the other regime $r_f < \xi$. Depending on the correlation length of the disorder, the system can thus cross over from one kind of dynamical behavior to another as the density is varied. In the first case, the pinning frequency and the threshold field increase with decreasing density. When the particle size exceeds the length scale of disorder, the pinning frequency and the threshold decrease with decreasing density. In both cases, the peak height decreases with decreasing density. This is compatible with the reduction of spectral weight with decreasing density. Such a crossover would lead to a maximum in the threshold field as the density is decreased.

If we now turn on a magnetic field perpendicular to the plane of the crystal, the result for Σ is unchanged as long as the magnetic length $l_c > \xi$. For weak fields, the peaks in the diagonal conductivity now occur at the frequencies $\omega_p^B = \omega_c \pm \omega_p^{B=0} \pm \frac{\omega_c^2}{8\omega_p^{B=0}}$. For strong enough fields such that $l_c \leq \xi$, we revert back to the usual strong field physics discussed in reference [21].

4.2 Surface acoustic wave measurements

Another physical property that can be extracted from our results pertains to surface acoustic waves (SAW). SAW measurements were used in the past to obtain the crystal dispersion relations [37]. In SAW measurements, the system is excited by a finite q SAW with a frequency $\omega = vq/2\pi$, where v is the velocity of the SAW. As the excitation traverses the system, the SAW propagation is completely affected by the piezoelectric interaction resulting in an attenuation and a shift in the SAW velocity. This shift δv and the attenuation rate κ are essentially determined by the density response function of the system and are given by [45]

$$\begin{aligned} \frac{\Delta v}{v} &= \frac{\alpha^2}{2} \frac{1}{1 + \left[\frac{\sigma(q)}{\sigma_m}\right]^2} \\ \kappa &= \frac{q\alpha^2}{2} \frac{\sigma(q)\sigma_m}{\sigma_m^2 + \sigma(q)^2} \end{aligned} \tag{53}$$

where α is the piezoelectric coupling constant which determines the interaction between the SAW and the electron system and $\sigma_m = v(\epsilon + \epsilon_0)$ where ϵ and ϵ_0 are the dielectric constants of the medium and vacuum respectively. and the momentum dependent longitudinal conductivity of the crystal $\sigma(q) \equiv \mathrm{Re}\sigma(q, \omega = vq)$. Notice that Δv and κ provide an indirect measurement of the conductivity at finite q. Using the results of the preceding sections, we obtain

$$\sigma(q,\omega) = \frac{i\rho_c^2 \omega q_x^2}{q^2} G_L(q,\omega) + \frac{i\rho_c^2 \omega q_y^2}{q^2} G_T(q,\omega) \tag{54}$$

where

$$\begin{aligned} G_L(q,\omega) &= \frac{1}{\Sigma + \Omega_L(q) - \rho_m \omega^2 + I(\omega)} \\ G_T(q,\omega) &= \frac{1}{\Sigma + \Omega_T(q) - \rho_m \omega^2 + I(\omega)}. \end{aligned} \tag{55}$$

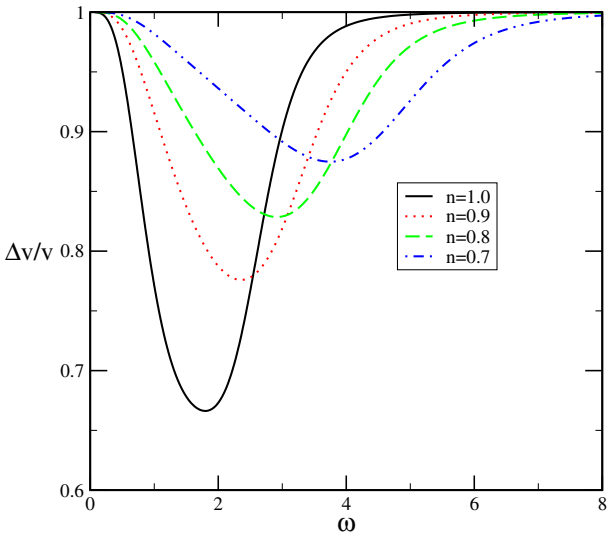

Fig. 4. The typical profile of the SAW velocity shift (in arbitrary units calculated for $\sigma_m = 1$ and $\alpha^2 = 2$) as a function of the frequency $\omega = vq$ and density. In both the regimes of disorder, the position of the minimum shifts to higher frequencies and the depth decreases as density is decreased. The quantitative behavior will be governed by the value of Σ. correlation length $r_f > \xi$. The curves are plotted for various values of the density n.

Using $I(\omega) = I_1(\omega) + iI_2(\omega)$ one gets

$$\mathrm{Re}\sigma(q, \omega = vq) = \frac{\rho_c^2 v}{q}\left[\frac{q_x^2 I_2(vq)}{[\Sigma + q^2(c_L - \rho_m v^2) + dq + I_1(vq)]^2 + I_2(vq)^2} + \frac{q_y^2 I_2(vq)}{[\Sigma + q^2(c_T - \rho_m v^2) + I_1(vq)]^2 + I_2(vq)^2}\right] \quad (56)$$

where I_1 and I_2 are the real and imaginary parts of $I(\omega)$. For small frequencies since $I_2(\omega) \propto \omega$, and Σ is the dominant scale,

$$\mathrm{Re}\sigma(q, \omega = vq) = \Gamma\frac{v^2 q^2}{\Sigma^2} \quad (57)$$

where $\Gamma = \sqrt{2\rho_m\Sigma[1 + \frac{4c_T\Sigma}{d^2}\log(\frac{d^2}{c_T\Sigma})]}$ is a density dependent parameter independent of q. Consequently, one has

$$\frac{\Delta v}{v} = \frac{\alpha^2}{2}\frac{1}{1 + \left[\frac{\Gamma v^2 q^2}{\Sigma^2\sigma_m}\right]^2}$$
$$\kappa = \frac{\alpha^2}{2}\frac{\Gamma v^2 q^3 \Sigma^2 \sigma_m}{\Sigma^4\sigma_m^2 + \Gamma^2 v^4 q^4}. \quad (58)$$

Using our results for $I(\omega)$ and the wave vector dependent conductivity, we can thus calculate the shift and attenuation for all values of q. The results are shown in Figure 4. In both the regimes $r_f \lessgtr \xi$, despite a reduction in the the magnitude of the SAW anomaly with decreasing density, the width of anomaly is expected to be strongly density dependent and is essentially dictated by the competition of the disorder scale r_f and the effective particle size. These results provide an impetus for detailed SAW experiments in the 2d electron gas systems. We reiterate that the above derivation has been done with the classical values of the elastic constants, and is thus valid deep in the crystal phase. A full quantitative prediction would require a precise knowledge of the variation of the elastic constants with density, a piece of information missing at the moment.

4.3 Power radiated by the 2d crystal

Another possible probe of the physics of the electron gas concerns thermometry. This involves a study of transfer of heat generated by a current in the electron gas to its three dimensional environment. This occurs via phonon emission at any given temperature and is related to the internal dynamics of the electron gas. These measurements were done on the electron gas both in the absence and presence of magnetic fields [46–48]. The expression for the power radiated by the 2d gas at a temperature T into cooler environment, considered to be at zero temperature is given by [47]:

$$P = \sum_{\mathbf{Q}} \omega(\mathbf{Q})|M(\mathbf{Q})|^2 n_B(\beta\hbar\omega(\mathbf{Q}))G(q, \omega(\mathbf{Q})) \quad (59)$$

where $G(q, \omega) \propto \omega\mathrm{Re}(1/\sigma(q, \omega))$, q is the projection of the phonon momentum $\mathbf{Q}$ onto the plane of the WC, M is the electron phonon matrix element and n_B is the usual Bose distribution function. Following reference [46], we assume that the electron phonon coupling is dominated by the piezoelectric effect and $|M(\mathbf{Q})|^2 \sim 1/Q$. In the absence of any external field and for high mobility systems, $G \propto \omega^2$ for $\omega \equiv \omega(\mathbf{Q}) \propto Q$ and and the predicted power radiated $P \propto T^5$ was found to be in accord with experiments. Based on power counting arguments, it was also shown that the radiated power in the IQHE phase $P \propto T^4$. In the light of these experiments, an obvious question is what is the power radiated in the pinned crystal. A naive approach would be to suppose that finite temperature contributions to $\mathrm{Re}1/\sigma$ are small at low temperatures, hence permitting one to approximate $G(q, \omega)$ by its zero temperature value. In this case, we find that for the frequency range $0 < \omega < \omega_p$, $\mathrm{Re}1/\sigma(q, \omega(q))$ does not vary significantly. Following the lines of references [46,47], since the typical values of wave vectors and frequencies of the phonons are small compared to the scales over which the inverse conductivity changes, we replace $G \propto \omega$. Again a simple power counting results in $P \sim T^4$ akin to what is seen in the IQHE phases.

A real calculation of P requires a knowledge of the finite temperature conductivity. At low enough temperatures, topological defects are thermally excited and they constitute the primary contribution to the ultra-low frequency conductivity. Though our formalism cannot treat the defects, we present heuristic arguments to justify our above result. A reasonable hypothesis for

the low temperature frequency dependent conductivity, is $\sigma(q,\omega,T) \sim \sigma(q,\omega,0) + \sigma_d(q,\omega,T)$, where σ_d is the defect contribution. The presence of σ_d leads to a finite but small dc conductivity $\sigma(T)$ in the long wavelength limit. We expect this to be the dominant contribution for small frequencies $\omega < \omega_d$ and for frequencies $\omega > \omega_d$, we expect the finite frequency contribution to dominate. The cut-off frequency ω_d is fixed by $\sigma(\omega, T = 0) \sim \sigma_d(T)$. Since for small frequencies, $\sigma(\omega, T = 0) \sim A\omega^2$, we obtain $\omega_d = \sqrt{\sigma_d(T)/A}$. This leads to the form that $\mathrm{Re}(1/\sigma(q,\omega,T) \sim \frac{1}{\sigma_d(T)} + Re(1/\sigma(q,\omega,T = 0)$. Using this form in (59), and doing the usual power counting, we obtain $P \propto T^4 + aT\sqrt{\sigma_d(T)}$. Since in the limit of low temperatures $\sigma_d(T)$ is expected to be exponentially small, the power spectrum is dominated by the T^4 term, thereby justifying our naive analysis of the preceding paragraph. This coincidence is related to the fact that both the pinned crystal and the IQHE phases are incompressible. Clearly, the variations seen in the inverse conductivity will modify this result, but we expect the result to hold for some range of low enough temperatures with a crossover to a different scaling form at higher temperatures.

5 Conclusions and experimental propositions

Before we conclude, we delve into the possibility of obtaining quantitative estimates for the theoretical scales R_a and Σ in the so called WC phase. These are very important for a real comparison of theoretical predictions with experimental data. The available experimental data which include mobility and resistivity measurements, permits one to calculate basic quantities like the the fermi momentum k_F and scattering rates. The fermi momentum can be expressed as a simple function of density $\pi a^2 = n$ or $r_s = a/a_B$, the mass renormalization factor m_r and the relative permittivity ϵ_r of the material. The Bohr radius of the electron in the given material is $a_B = \epsilon_r/m_r 0.53$ Å. Using the relation for the Fermi energy of the electron gas, $E_F = \frac{\hbar^2}{m^* a^2} \equiv \hbar^2 k_F^2/m^*$, one finds

$$k_F = 1.768 n^{\frac{1}{2}} \simeq \frac{m_r}{\epsilon_r r_s} 1.88 \times 10^{10} \tag{60}$$

k_F is expressed in units of inverse meters. We also find that the plasma frequency of the electron gas

$$\omega_{plas}^2 = \frac{e^2}{2\pi m^* \epsilon a^3} \tag{61}$$

and the pinning frequency $\omega_p = \sqrt{\frac{c_T}{\rho_m}} R_c^{-1}$ which as shown earlier, sets the scale for the conductivity and other dynamical quantities, satisfy the following relation

$$\frac{\omega_{plas}}{\omega_p} \sim \frac{R_c}{\sqrt{2}a} \tag{62}$$

where, the Larkin length $R_c \simeq R_a[\xi_0/a]^3$. Since most experiments on the 2D electron gas in Si MOSFETS and clean heterojunctions probe dc quantities, they cannot permit a simple extraction of the disorder scales. To use the available data on dc transport to extract the disorder scales, would require a detailed theoretical study of finite temperature dc transport, which is clearly beyond the scope of this paper and that of the variational method. The only other possibility is through measurements of microwave conductivity which presents a straightforward way of extracting the pinning frequency. These measurements in conjunction with SAW measurements which can be used to obtain the effective elastic modulus can then be combined with theoretical studies to verify the collectively pinned nature of the crystal.

To conclude, in this paper, we have studied the the physical properties of the Wigner crystal of a low density electron gas that is pinned by weak Gaussian disorder. We have used the standard combination of the Gaussian variational method and replicas to calculate a host of transport properties. We presented results for the evolution of the dynamical conductivity as a function of density in both the regimes where the effective particle size ξ is bigger or smaller than the disorder correlation length r_f, the SAW attenuation and the putative power radiated by the pinned crystal to its environment. We hope that our results provide a stimulus for microwave conductivity measurements which have been instrumental in establishing the crystalline nature of the 2DEG in very strong magnetic fields [23]. This will then instigate a real debate as to whether the insulating phase seen in systems which exhibit the 2d MIT is really a Wigner crystal or some other phase.

Clearly many questions still need to be addressed in order to understand the real nature of the crystalline state. As mentioned earlier, one first needs to evaluate the elastic constants of the crystal as a function of the density. The variational wave function used in the Section 2.1 to obtain the effective particle size can be used to obtain reasonable estimates of these constants. We expect the bulk modulus to not differ much from the result of reference [26] since this is fixed solely by the coulomb interaction. However, the shear modulus is bound to deviate from the classical value especially as it approaches melting when the density is varied. These values when plugged into the results obtained in this paper can lead to a behavior, not too far from the melting of the crystal, which deviates strongly from that expected for a system with the classical elastic constants. Secondly, in the absence of a strong magnetic field, the spinful nature of the electrons might lead to interesting spin physics in the crystalline phase. Interesting spin liquid behaviors have been seen in studies of the multi- exchange spin models in a triangular lattice [49,50] and it would be pertinent to ask if such exotic spin physics arises in the crystal and how does this change when the system is pinned by the incipient disorder. Moreover, any theoretical study of the magneto-resistance needs to take the spin physics into account. Other questions concern the behavior of the system close to depinning as also the dc transport at finite temperature. Some of these questions will be addressed in future work.

This work was supported in part by the Swiss National Fund through Manep and Division II and a French ACI grant.

Appendix A: RPA

A standard way to compute the compressibility of a charged system is through the free energy F of the system assuming neutrality, and from that to compute $d\mu/dN$. Since the system is always supposed to remain neutral the compressibility stays finite even for a charged system. However, this method is cumbersome since the calculation of the free energy is usually more difficult than that of a correlation function. In this appendix we show, using the RPA approximation, that the formula (23) indeed yields the standard results for the compressibility of a normal metal.

Using (22) it is easy to check that the susceptibilities $\chi_{\alpha\beta} = \langle \rho_\alpha \rho_\beta \rangle$ are given, in RPA, by

$$\begin{pmatrix} \chi_{11} \\ \chi_{12} \end{pmatrix} = - \begin{pmatrix} \chi^0 V_{11} & \chi^0 V_{12} \\ \chi^0 V_{12} & \chi^0 V_{11} \end{pmatrix} \begin{pmatrix} \chi_{11} \\ \chi_{12} \end{pmatrix} + \begin{pmatrix} \chi^0 \\ 0 \end{pmatrix} \quad \text{(A.1)}$$

where χ^0 is the bare (i.e. for H^0 only) density-density correlation function in one of the systems and the q and ω dependence is implicit. It is easy to solve (A.1) to obtain the (q dependent) capacitance

$$\chi_{11}(\omega, \mathbf{q}) - \chi_{12}(\omega, \mathbf{q}) = \frac{\chi^0(\omega, \mathbf{q})}{1 + \chi^0(\omega, \mathbf{q})(V_{11}(\mathbf{q}) - V_{12}(\mathbf{q}))}. \quad \text{(A.2)}$$

The Fourier transform of the Coulomb potentials are given by (31). The true capacitance corresponds to $\omega = 0$ and the limit $q \to 0$ which leads to

$$C = \frac{1}{(2\chi^0(q=0))^{-1} + 4\pi d}. \quad \text{(A.3)}$$

The total capacitance is thus the sum of a geometrical one C_{geom} and one due to the electron gas residing in the planes C_{el}

$$\frac{1}{C} = \frac{1}{C_{\text{geom}}} + \frac{1}{C_{\text{el}}}. \quad \text{(A.4)}$$

The geometrical one is the standard $1/(4\pi d)$ result. For a simple electron gas, $\chi^0(q=0)^{-1}$ is simply the screening length λ. One thus recovers that the geometrical distance d between the planes is effectively enhanced by the electronic screening length λ on each plane.

Appendix B: Calculation of the elastic coefficients

The decomposition of the density (10) allows to recover quite simply the formulas of reference [26] for the elastic coefficients. Indeed if one assumes that the interaction between the particles of the crystal is

$$H = \frac{1}{2} \int_{\mathbf{r},\mathbf{r}'} V(\mathbf{r} - \mathbf{r}')[\rho(\mathbf{r}) - \rho_0][\rho(\mathbf{r}') - \rho_0] \quad \text{(B.1)}$$

where $V(\mathbf{r} - \mathbf{r}')$ is the (three dimensional) Coulomb interaction. The decomposition of the density (10) allows us to rewrite (B.1) as

$$H = \frac{\rho_0^2}{2} \int_{\mathbf{r},\mathbf{r}'} V(\mathbf{r} - \mathbf{r}')[\nabla \cdot \mathbf{u}(\mathbf{r})][\nabla \cdot \mathbf{u}(\mathbf{r}')] + \frac{\rho_0^2}{2} \sum_{\mathbf{K} \neq 0} \int_{\mathbf{r},\mathbf{r}'} V(\mathbf{r} - \mathbf{r}') e^{i\mathbf{K}\cdot(\mathbf{r}-\mathbf{r}')} e^{-i\mathbf{K}\cdot(\mathbf{u}(\mathbf{r})-\mathbf{u}(\mathbf{r}'))} \quad \text{(B.2)}$$

where we have only kept terms that are not averaged to zero due to the translational invariance. The first term in (B.2) gives back the term proportional to q in (8). Indeed one obtains

$$H_1 = \frac{1}{2\Omega} \sum_{\mathbf{q}} \frac{e^2 \rho_0^2 q}{\epsilon} u_L^*(\mathbf{q}) u_L(\mathbf{q}). \quad \text{(B.3)}$$

This gives the value $d = \rho_c^2/\epsilon$.

The second term can be expanded to second order in u to give the elastic coefficients. The first order term vanishes because the perfect lattice ($u = 0$) is an extremum of the energy. Up to second order in u,

$$H_2 = \frac{\rho_0^2}{2} \sum_{\mathbf{K} \neq 0} \int_{\mathbf{r},\mathbf{r}'} V(\mathbf{r} - \mathbf{r}') e^{i\mathbf{K}\cdot(\mathbf{r}-\mathbf{r}')} K_\alpha K_\beta \times (u_\alpha(\mathbf{r}) - u_\alpha(\mathbf{r}'))(u_\beta(\mathbf{r}) - u_\beta(\mathbf{r}')) \quad \text{(B.4)}$$

where the summation on the coordinate indices α, $\beta = (x, y)$ is implicit. Using

$$u_\alpha(\mathbf{r}) - u_\alpha(\mathbf{r}') = \frac{1}{\Omega} \sum_{\mathbf{q}} u_\alpha(\mathbf{q}) \left(e^{i\mathbf{q}\cdot\mathbf{r}} - e^{i\mathbf{q}\cdot\mathbf{r}'} \right). \quad \text{(B.5)}$$

One can rewrite (B.4) as

$$H_2 = \frac{\rho_0^2}{2\Omega^2} \sum_{\mathbf{K} \neq 0} \sum_{\mathbf{q},\mathbf{q}'} \int_{\mathbf{r},\mathbf{r}'} V(\mathbf{r} - \mathbf{r}') e^{i\mathbf{K}\cdot(\mathbf{r}-\mathbf{r}')} K_\alpha K_\beta u_\alpha(\mathbf{q}) u_\beta(\mathbf{q}') \left(e^{i\mathbf{q}\cdot\mathbf{r}} - e^{i\mathbf{q}\cdot\mathbf{r}'} \right) \left(e^{i\mathbf{q}'\cdot\mathbf{r}} - e^{i\mathbf{q}'\cdot\mathbf{r}'} \right). \quad \text{(B.6)}$$

Using center of mass $\mathbf{R} = \mathbf{r} + \mathbf{r}'$ and relative $\mathbf{r}_0 = \mathbf{r} - \mathbf{r}'$ coordinates can be rewritten as

$$H_2 = \frac{\rho_0^2}{2\Omega} \sum_{\mathbf{K} \neq 0} \sum_{\mathbf{q}} \int_{\mathbf{r}_0} V(\mathbf{r}_0) e^{i\mathbf{K}\cdot\mathbf{r}_0} K_\alpha K_\beta u_\alpha(\mathbf{q}) u_\beta(-\mathbf{q}) \times (2 - 2\cos(\mathbf{q} \cdot \mathbf{r}_0)) \quad \text{(B.7)}$$

which using the Fourier transform of the potential $V(r_0)$ denoted $\tilde{V}(\mathbf{q}) = 1/q$ one obtains

$$H_2 = \frac{\rho_0^2}{2\Omega} \sum_{\mathbf{q}} \left[\sum_{\mathbf{K} \neq 0} K_\alpha K_\beta (2\tilde{V}(\mathbf{K}) - \tilde{V}(\mathbf{K} + \mathbf{q}) - \tilde{V}(\mathbf{K} - \mathbf{q}) \right] u_\alpha(\mathbf{q}) u_\beta(-\mathbf{q}) \quad \text{(B.8)}$$

which gives the classical elastic constants.

References

1. E. Abrahams, S.V. Kravchenko, M.P. Sarachik, Rev. Mod. Phys. **73**, 251 (2001)
2. P.W. Anderson, Phys. Rev. **109**, 1492 (1958)
3. E. Abrahams, P.W. Anderson, D.C. Licciardello, T.V. Ramakrishnan, Phys. Rev. Lett. **42**, 673 (1979)
4. P.A. Lee, T.V. Ramakhrishnan, Rev. Mod. Phys. **57**, 287 (1985)
5. A.M. Finkelstein, Z. Phys. B **56**, 189 (1984)
6. For a review see: D. Belitz, T.R. Kirkpatrick, Rev. Mod. Phys. **66** 261 (1994)
7. A.O. Gogolin, A.A. Nersesyan, A.M. Tsvelik, *Bosonization and Strongly Correlated Systems* (Cambridge University Press, Cambridge, 1999)
8. T. Giamarchi, *Quantum Physics in One Dimension* (Oxford University Press, Oxford, 2004)
9. T. Giamarchi, H.J. Schulz, Phys. Rev. B **37**, 325 (1988)
10. E. Wigner, Phys. Rev. **46**, 1002 (1934)
11. D. Ceperley, Phys. Rev. B **46**, 1002 (1984)
12. H. Fukuyama, P. Lee, Phys. Rev. B **18**, 6245 (1978)
13. G. Blatter, M.V. Feigel'man, V.B. Geshkenbein, A.I. Larkin, V.M. Vinokur, Rev. Mod. Phys. **66**, 1125 (1994)
14. T. Nattermann, S. Scheidl, Adv. Phys. **49**, 607 (2000)
15. T. Giamarchi, S. Bhattacharya, in *High Magnetic Fields: Applications in Condensed Matter Physics and Spectroscopy*, edited by C. Berthier et al. (Springer-Verlag, Berlin, 2002), p. 314, `cond-mat/0111052`
16. T. Giamarchi, E. Orignac, in *Theoretical Methods for Strongly Correlated Electrons*, edited by D. Sénechal et al. (Springer, New York, 2003), CRM Series in Mathematical Physics, `cond-mat/0005220`
17. T. Giamarchi, *Quantum phenomena in mesoscopic system* (IOS Press, Amsterdam, 2003), `cond-mat/0403531`
18. B.G.A. Normand, P.B. Littlewood, A.J. Millis, Phys. Rev. B **46**, 3920 (1992)
19. R. Chitra, T. Giamarchi, P. Le Doussal, Phys. Rev. Lett. **80**, 3827 (1998)
20. H.M. Yi, H.A. Fertig, Phys. Rev. B **61**, 5311 (2000)
21. R. Chitra, T. Giamarchi, P. Le Doussal, Phys. Rev. B **65**, 035312 (2001)
22. M.M. Fogler, D.A. Huse, Phys. Rev. B **62**, 7553 (2000)
23. C.C. Li, L.W. Engel, D. Shahar, D.C. Tsui, M. Shayegan, Phys. Rev. Lett. **79**, 1353 (1997)
24. C.C. Li, J. Yoon, L.W. Engel, D. Shahar, D.C. Tsui, M. Shayegan, Phys. Rev. B **61**, 10905 (2000)
25. S. Chakravarty, S. Kivelson, C. Nayak, K. Voelker, Phil. Mag. B **79**, 859 (1999)
26. L. Bonsall, A.A. Maradudin, Phys. Rev. B **15**, 1959 (1977)
27. T. Giamarchi, P. Le Doussal, Phys. Rev. Lett. **72**, 1530 (1994)
28. T. Giamarchi, P. Le Doussal, Phys. Rev. B **52**, 1242 (1995)
29. T. Giamarchi, P. Le Doussal, Phys. Rev. B **53**, 15206 (1996)
30. T. Giamarchi, P. Le Doussal, *Statics and dynamics of disordered elastic systems* (World Scientific, Singapore, 1998), p. 321, `cond-mat/9705096`
31. A.I. Larkin, Y.N. Ovchinnikov, J. Low Temp. Phys. **34**, 409 (1979)
32. J.P. Eisenstein, L.N. Pfeiffer, K.W. West, Phys. Rev. Lett. **68**, 674 (1992)
33. T. Giamarchi, in *Strongly correlated fermions and bosons in low dimensional disordered systems*, edited by I.V. Lerner et al. (Kluwer, Dordrecht, 2002), `cond-mat/0205099`
34. V.I. Falko, Phys. Rev. B **49**, 7774 (1994)
35. T.T. Nguyen, A.Y. Grosberg, B.I. Shklovskii (2001), `cond-mat/0101103`
36. Y.P. Li et al., Solid State Commun. **95**, 619 (1995)
37. E.Y. Andrei, G. Deville, D.C. Glattli, F.I.B. Williams, Phys. Rev. Lett. **60**, 2765 (1988)
38. F.I.B. Williams, P.A. Wright, R.G. Clark, E.Y. Andrei, G. Deville, D.C. Glattli, O. Probst, B. Etienne, C. Dorin, C.T. Foxon et al., Phys. Rev. Lett. **66**, 3285 (1991)
39. H. Fukuyama, P.A. Lee, Phys. Rev. B **17**, 535 (1978)
40. C. Zeng, P.L. Leath, D.S. Fisher, Phys. Rev. Lett. **82**, 1935 (1999)
41. P. Le Doussal, T. Giamarchi, Physica C **331**, 233 (2000)
42. B.I. Shklovskii, A.L. Efros, Sov. Phys. JETP **54**, 218 (1981)
43. B.I. Shklovskii, Phys. Stat. Sol. (c) **1**, 46 (2004)
44. T. Nattermann, T. Giamarchi, P. Le Doussal, Phys. Rev. Lett. **91**, 056603 (2003)
45. B.I. Halperin, P.A. Lee, N. Read, Phys. Rev. B **47**, 7312 (1993)
46. E. Chow, H.P. Wei, S.M. Girvin, M. Shayegan, Phys. Rev. Lett. **77**, 1143 (1996)
47. E. Chow, H.P. Wei, S.M. Girvin, W. Jan, J. Cunningham, Phys. Rev. B **56**, 1676 (1997)
48. N.J. Appleyard, J.T. Nicholls, M.Y. Simmons, W.R. Tribe, M. Pepper, Phys. Rev. Lett. **81**, 3491 (1998)
49. G. Misguich, C. Lhuillier, B. Bernu, C. Waldtmann, Phys. Rev. B **60**, 1064 (1999)
50. K. Voelker, S. Chakravarty, Phys. Rev. B **64**, 235125 (2001)